



Received 14 September 2022; revised 9 November 2022; accepted 2 December 2022. Date of publication 26 December 2022; date of current version 7 April 2023.

Digital Object Identifier 10.1109/JMW.2022.3227242

# Improving Isolation in Monostatic Simultaneous Transmit and Receive Systems Using a Quasi-Symmetrical Self-Interference Cancellation Architecture

MD NURUL ANWAR TAREK (Graduate Student Member, IEEE),
MARISOL ROMAN GUERRA (Graduate Student Member, IEEE),
ANTHONY NUNEZ (Graduate Student Member, IEEE),
MD NAZIM UDDIN (Graduate Student Member, IEEE), AND ELIAS A. ALWAN (Member, IEEE)

(Regular Paper)

Department of Electrical Engineering, Florida International University, Miami, FL 33174 USA CORRESPONDING AUTHOR: Md Nurul Anwar Tarek (e-mail: mtare002@fiu.edu).

This work was supported in part by the National Science Foundation (NSF) under Award #1943040, and in part by the NASA OSE Fellowship under Grant #80NSSC20K1463

**ABSTRACT** For simultaneous transmit (Tx) and receive (Rx), it is a common practice, with monostatic full duplex (FD) systems, to use a single antenna and a circulator to provide isolation between the transmit and receive radio chains. However, most circulators currently on the market are designed to provide 12 to 20 dB of Tx/Rx port isolation, which is not sufficient for full duplex (FD) microwave communication. In fact, it is necessary to provide at least >30 dB of isolation to prevent the receiver desensitization that is caused by the leakage of high-power transmit signals. For this reason, practical simultaneous transmit and receive (STAR) systems require additional cancellation stages. In this paper, we present a novel STAR system that incorporates two circulators, a hybrid coupler, and a self-interference cancellation (SIC) circuit, based on a Finite Impulse Response (FIR) topology. Our design achieves an average Tx/Rx port isolation of  $\sim$ 37 dB over a 25 MHz bandwidth (viz. 2.395–2.42 GHz) in simulation, with a minimum and maximum cancellations of 35 dB and 41 dB, respectively. A prototype was fabricated and tested showing good agreement with the simulations. All in all, the prototype achieved an average cancellation of 36 dB, with a cancellation range of 33 dB to 42 dB.

**INDEX TERMS** Coupling signal, in-band full duplex (IBFD), simultaneous transmit and receive (STAR), self-interference cancellation (SIC).

### I. INTRODUCTION

Current communication systems have operated in a mutually exclusive manner, requiring either two frequency bands to operate simultaneously (i.e., Frequency Division Duplexing, FDD) or two time slots to operate on the same band (i.e., Time Division Duplexing, TDD) [1], [2]. In contrast full duplex (FD) systems presents an efficient use of time-frequency resources by enabling simultaneous transmission (Tx) and reception (Rx) in the same frequency band. The successful

operation of FD system requires high isolation between the Tx and Rx chains to avoid high power Tx signals from leaking into the receiver and desensitizing it. However, with the rise and development of 5G and 6G technologies [3], [4], [5], systems able to simultaneous transmit and receive, and hence double the spectral efficiency, have become a necessity with the remarkably congested Radio Frequency (RF) spectrum. As such, STAR systems with high Tx/Rx isolation [6] is a challenge that must be tackled swiftly to alleviate the

overcrowded RF spectrum. A failure to do so implies an increased spectral vulnerability to signal fratricide and interference, as well as falling short to accommodate the growing number of users, of both humans and connected machines.

Foremost, FD designs can be classified into two categories, monostatic or bistatic [7], [8], [9]. The monostatic designs share an antenna for both transmitting and receiving. Ultimately, this configuration relies on circulators and antennas, with high isolation capabilities, to cancel out the self-interference (SI). On the other hand, bistatic designs require separate antennas for transmit and receive. Given the need for multiple antennas, bistatic designs achieve the cancellation of the coupling through spacing, polarization, beam squint diversity, and other techniques. Nevertheless, several research indicate that multiple cancellation stages must be implemented in the analog and digital domains to target SI and achieve the desired isolation levels [10], [11], [12] for both monostatic and bistatic FD designs. In fact, across the STAR literature, most works, [13], [14], have recognized the following as the main stages for SIC: (1) the antenna stage, which involves making space or design modifications to the physical antenna to reduce the coupling between the transmit and receive antennas; (2) the RF stage, which involves implementing RF SIC circuits; and (3) the digital stage, which involves the use of probabilistic channel models.

As already mentioned, bistatic designs require at least one Rx antenna and one Tx antenna to achieve a higher level of isolation by adjusting the spacing between these antennas. As a result, this method often demands a significant distance between the Tx and Rx antennas. Therefore, it is impractical for many applications, such as the sub-6 GHz range or higher frequencies, where the space is limited [15]. For instance, in [16], an 8-element transmit ring antenna array, with an elevated Rx element on the circular ground plane, is designed. The system's Rx and Tx antennas achieve 55 dB of isolation, along with an omni-directional pattern, from 2.4 to 2.5 GHz through the use of a beamformer that phases the opposing parts 180° apart. However, this multi-in, multi-out approach is constrained by the amount of available space and leads to an overall unstable system efficiency. Additionally, as the number of Tx components rises, the beamformer network becomes more complicated and sensitive to feeding network flaws and size.

Other examples of techniques applied to bistatic designs include the placement of tunable resonators between the Tx and Rx antennas in order to reduce coupling, as shown in [17]. However, this approach also requires large separation, which is unfeasible for many applications with small space available. There is also a polarization multiplexing method to enable the co-location of Tx and Rx antennas. For instance, [18] demonstrates a wideband SIC cancellation system using a Tx/Rx antenna pair with orthogonal linear polarization. When the SIC circuit is turned on, it produces 50 dB isolation across a 300 MHz bandwidth centered at 4.6 GHz. Using polarization orthogonality is acceptable for commercial purposes. However, it is not suitable when full polarization diversity is

required, such as in military radios, including the evaluation of electronic warfare engagements. All in all, bistatic FD systems generally require large separation distance between the Tx and Rx antennas to provide high levels of isolation. On that account, monostatic FD systems are the most suited design for applications with space limits.

Despite being favorable for applications with small-sized devices, the reliance of monostatic systems on circulators and other components produce a different set of drawbacks. Foremost, these components have internal leakage and power losses, which lead to inadequate isolation and increased power consumption. For example, in [19], a wideband monostatic setup incorporates a Wilkinson power divider, two circulators, and a balun. This setup provides 45 dB isolation in the frequency range of 2-4 GHz. Even though, an acceptable isolation is achieved across a wide bandwidth, however, half of the Tx signal is lost in the process of creating the equivalent leaking signal for cancellation. Similarly, the circulator-free design accomplished with a 180° coupler and power splitters presented in [20], results in a loss of half the Tx power. In [21], a two-point SIC system is presented, which contributes to reducing the interference between the Tx and Rx in FD radios. This research was able to provide 50 dB of SIC across 42 MHz of bandwidth. However, this cancellation shows high power loss at the Tx chain. In addition due to use of a 19 tap filtering technique, the SIC circuit is complex. In another study, an integrated six-port beam forming network (BFN) is used to achieve 40 dB cancellation across 107 MHz. Since a BFN Network requires two 180° hybrid couplers, one 90° hybrid coupler, and one Wilkinson power divider, a 3 dB power loss is observed at the Tx chain [22]. In another research [23], a monastic circularly polarized antenna system is presented to provide 40 dB of cancellation across 100 MHz. In this work, the feeding technique requires several Wilkinson power divider implying high power loss at the Tx and Rx Chains. In [24], a BFN butter matrix is introduced in the Tx and Rx chains of a monostatic dual-polarized STAR antenna system. This study achieved 47 dB of isolation across a 100 MHz bandwidth. It should be noted that the butter matrix is implemented with three hybrid couplers, resulting in high power loss at both the Tx and Rx chains. Similarly, in [25], three quadrature hybrids were used to achieve 35 dB of isolation across a large bandwidth of 2.6 GHz. This method shows 4.5 dB insertion loss in both Tx and Rx chains. Another study [26] implemented impedance tuning circuit at the coupling port of a directional coupler. This design was able to achieve 65 dB of carrier leakage cancellation across a 100 MHz frequency band. However, because a directional coupler is used, a significant amount of Tx power is lost. Furthermore, tuning circuits are difficult to implement at high frequencies.

Alternatively, even with the implementation of an electrically balanced duplexer, as done in [27]-[28], there is still a significant amount of Tx insertion loss that results in half power loss of the Tx signal. In [14], a quadrature balanced power amplifier (QBPA) is used as SIC canceller





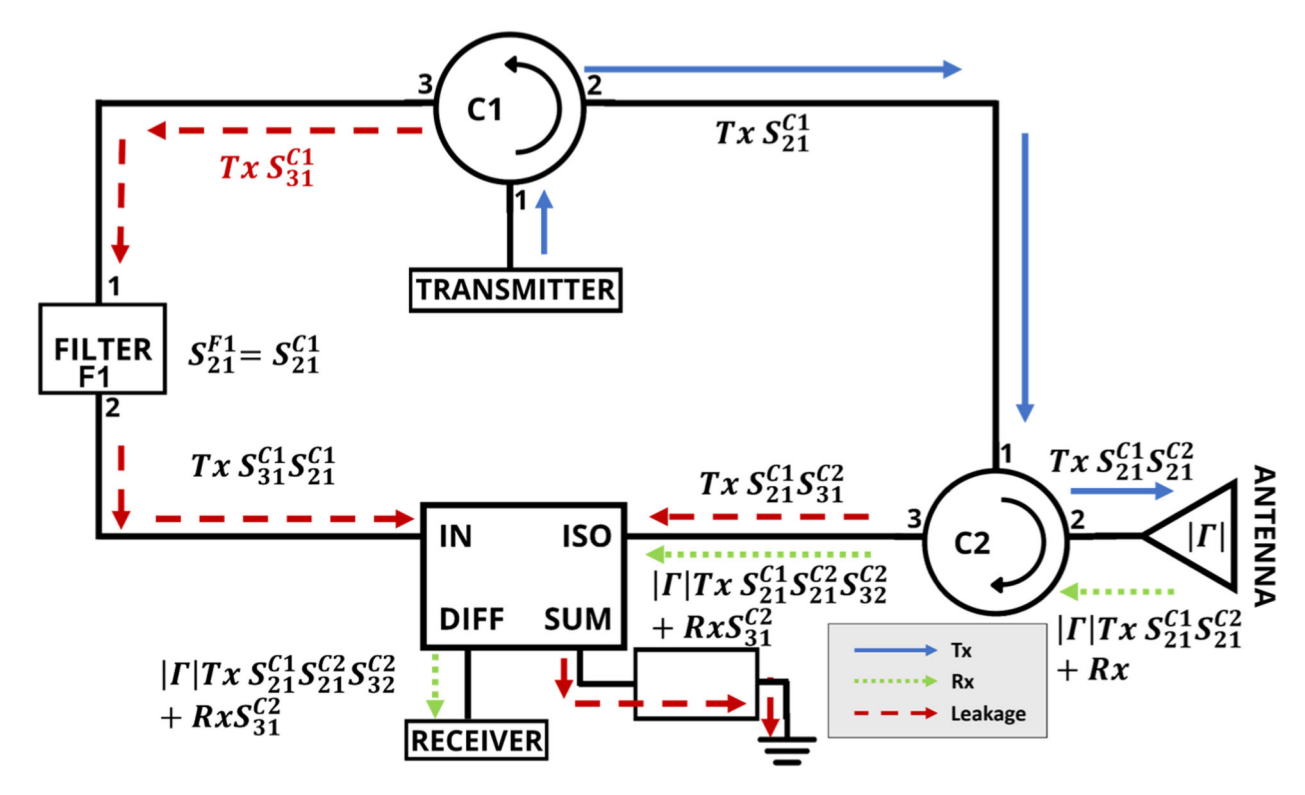


FIGURE 1. A monostatic dual circulator STAR system operating across 25 MHz. The architecture is composed of two circulator, FIR filter, and a hybrid coupler to achieve up to 42 dB of self-interference cancellation.

to improve Tx and Rx losses. However, this improvement was achieved at the cost of additional use of power amplifiers and hybrid couplers, implying increased hardware complexity.

Furthermore, the simple circulators structure realized in [29] achieved an isolation greater than 60 dB from 902-928 MHz with a circularly polarized patch antenna, a simple balanced feed network, and a second layer of analog feedforward cancellation circuitry. However, there is Tx loss when feeding the circulator. Another work using circulator has reported 40 dB cancellation across 65 MHz of bandwidth [30]. However, because the structure uses inductors and capacitors, components with a low-quality factor, it needs an impedance matching terminal, which is difficult to implement at higher frequencies [30]. In [31], a new photonic circulator with Tx/Rx isolation greater than 39.6 dB across a 10:1 bandwidth is presented. However, its performance rapidly degrades when the antenna is poorly matched. In addition, one of the potential drawbacks of photonic circulators is their lower power handling compared to the fertile circulator.

In this article, we present a monostatic STAR architecture, as shown in Fig. 1. This work is an extension of our previous research published in [32], which was solely based on simulation, whereas this paper features a fabricated prototype and brings forward several novelties, among them:

1) The RF-SIC system is power efficient as it achieves high isolation with a minimal power loss of the Tx signal, whereas other designs lose an additional 3 dB at both the

- Tx and Rx signal. In our design, there is no requirement for splitting the Tx signal.
- 2) The symmetrical design is simple, yet novel as it only requires two circulators and a finite impulse response (FIR) circuit topology to provide up to 42 dB in isolation across the operational bandwidth. The placement of the FIR circuit brings passive cancellation at the Rx chain where as other research requires active circuit such as IMT [30].
- The second circulator and the FIR filter enable the creation of a quasi-replica of the leaked transmitted signal for passive symmetric cancellation.
- 4) The addition of an FIR filter between the two circulators improves the secondary matching to approximate the channel coupling for further SIC.
- 5) The implementation of a differential evolution algorithm (DE) to optimize the FIR filter. This type of algorithm was selected because the optimization of the FIR filter in analog domain requires a high tuned solution and no initial guess. Moreover, DE it is a population-based optimizer for finding the best solution of a problem; in its most basic form, it is the process of adding the weighted difference between two population vectors to a third vector.

Consequently, our improved STAR architecture was able to achieve a minimum isolation of 35 dB and a maximum isolation of 41 dB in simulation. Similarly, the measurements of the fabricated prototype reached an isolation of 33 dB and

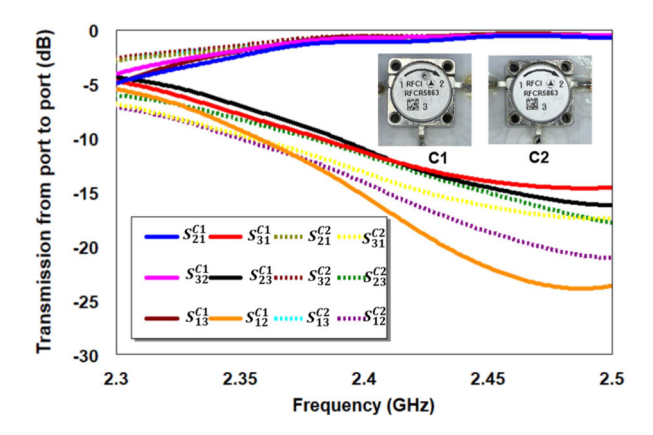


FIGURE 2. Transmission and isolation at the different ports for circulators C1 and C2.

42 dB, respectively, between the Tx and the Rx ports across 2.395–2.420 GHz.

This article is structured as follows: Section II describes the principle operation of the dual circulator monostatic SIC design. Section III shows the mathematical representation of the SIC. Section IV, describes the components in the monostatic STAR system and shows the antenna performance. Section V demonstrates the design process of the FIR circuit that allows for the symmetrical cancellation. Sections VI includes the fabricated prototype results and measurement setup, respectively. Section VII presents a comparison of our system with other state-of-the-art STAR implementations. Section VIII concludes the paper.

#### II. SELF-INTERFERENCE CANCELLATION ARCHITECTURE

We present a monostatic STAR system, shown in Fig. 1, consisting of two identical circulators (first circulator denoted as C1 and second circulator as C2), one customized finite impulse response (FIR) filter, and one 180° hybrid coupler. C2 and FIR filter are placed on the right and left sides of the first circulator, respectively, to create a symmetrical topology. The addition of C2 to the overall structure, along with the filter, allows us to pseudo-replicate the leaked transmitted signal from C2 and cancel it out. In this case, once the leaked signal from C1 is filtered, it matches the signal leaked from C2 that comes mixed with the Rx signal; correspondingly, the Rx signal can be smoothly separated from the leakage at the differential port of the hybrid coupler. It is noted that the most advantageous feature of this design is that the RF-SIC system is power efficient. There is minimal power loss in the Tx signal, whereas traditional approaches result in a 3 dB power loss at both the Tx and Rx ports. Adding a additional circulator results in only 0.707 dB insertion loss as shown in the measured result in Fig. 2. Consequently, transmission efficiency is high compared to the conventional approaches. As a result, this symmetrical setup leads to a high isolation with a minimal power loss of the Tx signal. While it must be noted that symmetry can also be achieved by adding a third circulator (C3), substituting it with an FIR filter brings less magnetic effect to the whole architecture. In addition, a customized FIR filter is able to provide better cancellation than the theoretical three-circulator system because the filter can be tunable (with variable gain and delay). In this work, we have limited the filter to a two-tapped FIR topology for ease of implementation. Although an additional tap can be included to improve rejection and achieve a wider stop-band, these stubs increase the physical dimension of the filter, making it unsuitable for low-profile antennas.

Overall, our design is compact and optimized across a 25 MHz bandwidth. The design of the entire system is presented first, followed by a detailed procedure of the RF cancellation from 2.395 to 2.420 GHz.

# III. ANALYSIS OF THE SYMMETRIC COUPLING CANCELLATION FOR THE RF STAGE

The STAR configuration, shown in Fig. 1, has most of the Tx signal going through the first circulator, C1, as  $TxS_{21}^{C1}$ , while a small fraction leaks,  $TxS_{31}^{C1}$ , due to the circulator's mismatches. Simultaneously, on the left side of the system, the leaked signal passes through the filter, F1. Notably, the filter design is based on a FIR circuit, which collectively behave as follows:

$$S_{21}^{F1} = S_{21}^{C1}. (1)$$

Therefore, at the output of the filter, the signal becomes:

$$TxS_{31}^{C1}S_{21}^{F1} = TxS_{31}^{C1}S_{21}^{C1}. (2)$$

Moreover, on the right portion of the system, the Tx signal,  $TxS_{21}^{C1}$ , is sent out to the antenna via C2. Meanwhile, some of the Tx signal leaks through port 3 of C2, adding to the incoming Rx signal and making the total signal:

$$y = TxS_{21}^{C1}S_{31}^{C2} + RxS_{32}^{C2}. (3)$$

It should be noted that both circulators are equivalent as shown below:

$$S_{31}^{C1} = S_{31}^{C2}. (4)$$

Therefore, the leaked Tx signals on the left and right sides are practically identical. As a result, the received signal,

$$RxS_{32}^{C2}$$
, (5)

is isolated at the difference port of the  $180^{\circ}$  hybrid coupler, where  $TxS_{21}^{C1}S_{31}^{C2}$  cancels out with the filtered quasi-replica,  $TxS_{31}^{C1}S_{21}^{C1}$ .

Using our method, the 3 dB loss in Tx signal is avoided, allowing us to maintain a satisfactory power level. Ideally, typical values of circulator/ isolator insertion loss are of the order 0.2 to 0.4 dB. It is important to note that since we have used commercially of the self (COTS) component, at the output of the first circulator, the insertion loss is 0.707 dB and at the output of the second circulator, the insertion loss for the Tx power is 1 dB. Therefore, the total insertion loss for the Tx power is 1.7 dB. Conversely, other designs show a 3 dB insertion loss. More details, on the antenna design and the SIC filter circuit, are provided in the following sections.





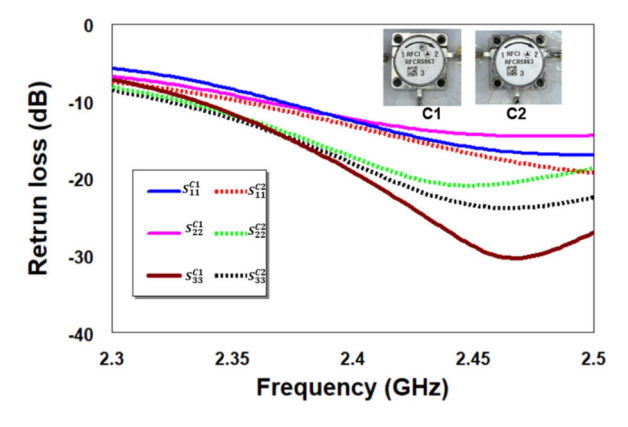


FIGURE 3. Return loss measurements of the circulators C1 and C2.

# IV. SEGMENTS OF THE SINGLE ANTENNA STAR SYSTEM A. CIRCULATORS

Within the framework of our topology, we have implemented two circulators, which resulted in a symmetrical design. Ideally, the responses of these two circulators ought to be identical because they are the same component. However, the measured responses of the two circulators actually varied. Therefore, since the isolation in monostatic systems will be limited by the performance of the circuit components, we must minimize the losses by reducing the number of components and picking high-performing options.

For this reason, we are only using two circulators from RFCI (component number CR5863). These circulators have an operating frequency range between 2.365–2.435 GHz. According to our measurements, the circulators have an isolation level of 15.5 dB at 2.41 GHz across all of the ports. The two key S-parameters, isolation and transmission, of each circulator were measured and shown in Fig. 2. Moreover, Fig. 3 shows the measured return loss at every port of the two circulators.

### B. ANTENNA

To test the antenna port and its corresponding leakage cancellation, a planar patch antenna was designed. We selected a patch as the most suitable design because it could be easily scaled to different bandwidths for testing and still shows a good match. Moreover, this antenna's characteristics, such as being light-weight, low-profile, portable, and fabrication-flexible, were advantageous for fabrication and measurement setup.

In this case, given that the circulators operate from 2.365 to 2.435 GHz, the antenna was designed for 2.4 GHz. Foremost, this cup-like antenna originally consisted of a rectangular  $58.48 \times 36.60$  mm<sup>2</sup> patch. However, an arc-shaped transition, with radius 32.9 mm, between the bottom half edges of the patch and the feed was added. The created round edges allow for smoother current flow and better matching across a wide bandwidth. Similarly, the antenna has a reduced ground plane, 39.55 mm long, with a notch, 5.95 mm deep, parallel to the feed, in order to reduce the Q-factor and achieve wideband

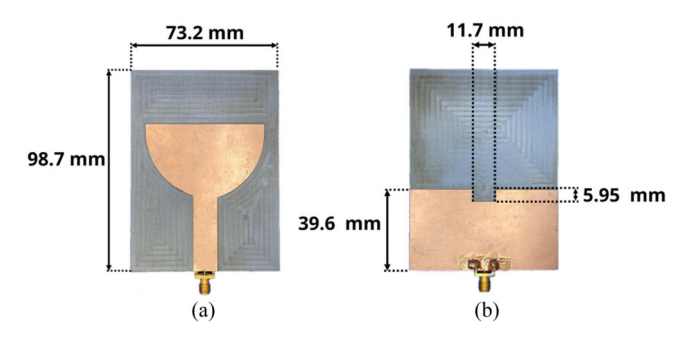
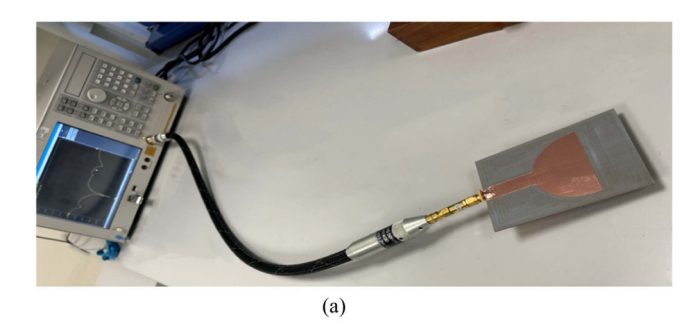


FIGURE 4. Geometry of the planar patch antenna. (a) Top view. (b) Bottom view



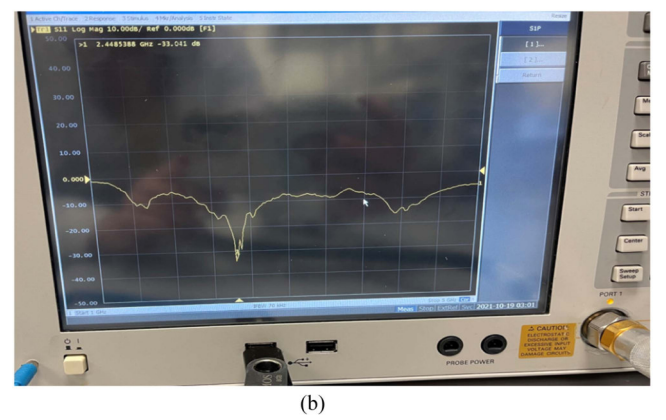


FIGURE 5. Measurement setup for the antenna. (a) VNA and the antenna. (b) Close-up of the VNA results.

operation. This prototype was printed on the RT/Duroid 5880 substrate ( $\epsilon_r = 2.2$  and  $\tan \delta = 0.009$ ) with a 1.575 mm thickness. Overall, the antenna, displayed in Fig. 4, is 73.2 × 98.7 mm<sup>2</sup>. Notably, the antenna design results taken with the Vector Network Analyzer (VNA), shown in Fig. 5, demonstrate a good match with the full-wave simulation, as shown in Fig. 6.

## C. FIR CIRCUIT

The physical architecture of the FIR filter is depicted in Fig. 7. For ease of fabrication, we chose to design a 2nd order FIR filter. Since the order of the filter is determined by the number of taps, this filter consists of a two-tapped FIR circuit that also includes delay lines and attenuators. Its design operates at 2.4 GHz and is based on the factors discussed in the following Section V of this article.

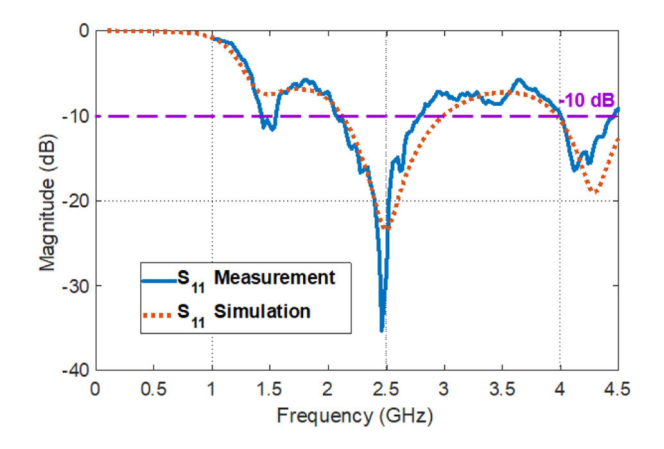


FIGURE 6. Simulated and measured S<sub>11</sub> of the antenna shown in Fig. 4.

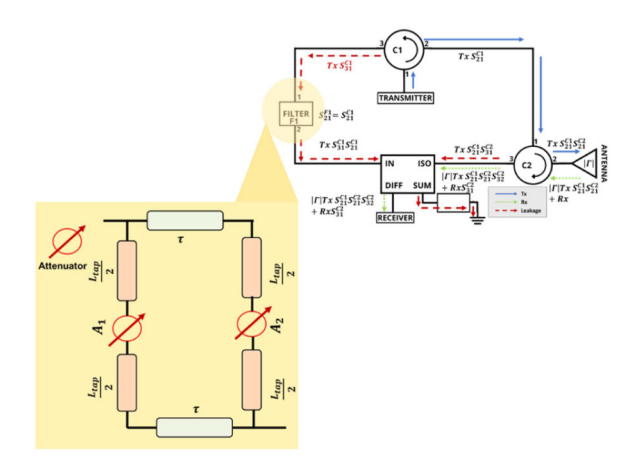


FIGURE 7. A Two-tap FIR circuit with delay lines and attenuators.

## V. SELF-INTERFERENCE CANCELLATION CIRCUIT DESIGN

This section investigates the two-tap FIR arrangement, which mimics the behavior of the circulator C1 transmission from port 1 to port 2. In an ideal situation, taking into account the identical operation of the two circulators, The transmission of C1 should satisfy (3). In reality, there is a small variation in the responses of the two circulators, as can be seen in Fig. 2. One of the advantages of using an FIR circuit is that it is able to compensate for these slight circulator mismatches in order to achieve the desired level of cancellation. Notably, we present a simple FIR circuit with a two-tap topology. the latter offers three degrees of freedom, one of which is the delay line, while the other two are the attenuators. As such, by varying these 3 degrees of freedom, we are able to match the leakage and modify possible frequency response discrepancies of the circuit components. As a result, this freedom allows the circuit to accomplish the required cancellation.

Fig. 7 shows the schematic of the presented FIR circuit with one delay line and two-tap coefficients. Each tap consists of one attenuator. In analog domain, the tap delays are represented by microstrip lines and the tap coefficients are realized with attenuators. The width and length of the delay lines and attenuators are optimized to achieve a transfer function that

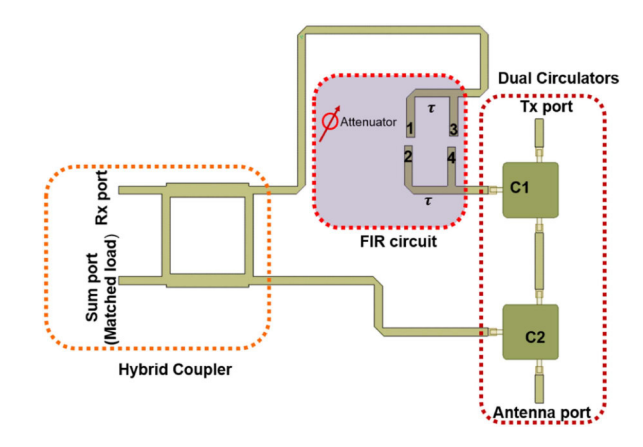


FIGURE 8. EM layout of the FIR circuit. Here is noted that the attenuator is a lumped component. One attenuator is later placed between port 1 and 2 and other one is placed between port 3 and 4, respectively.

is matched to the Tx signal passed by circulator C1. It must be noted that the FIR circuit is also a function of C2 given that it is the same as C1. Overall, the design of the FIR circuit response takes into consideration both circulators' responses.

The electromagnetic (EM) layout of our architecture is depicted in Fig. 8. The delay lines and attenuators were optimized to achieve a filter response that satisfied (2) and (3). In other words, the FIR circuit played a crucial role in capturing the dual circulator effect by adjusting the gain delay of the attenuators and the transmission lines (copper traced), respectively, across the desired frequency band of 2.395-2.42 GHz.

We note that, from the basic network, the passive multi-port networks corresponding to circulator leakage effect contain transfer functions (TFs) with both zeros and poles in their integer-order polynomial representations. The approximation of such coupling functions using FIR circuit is possible. Here, our architecture was fabricated on a microstrip substrate to keep the circuit low profile. To reproduce this network's unit impulse response, an FIR filter would need to sample it at close intervals of time and use the sampled values as weights (viz. taps) for the FIR realization. The TF of the FIR filter can be represented using circuit taps, which are implemented using tap delay lines and tap coefficients. In this two tapped FIR circuit each tapped length is 24 mm. The form factor of this FIR circuit is 16 mm  $\times$  24 mm.

More in detail, we designed a 2th order circuit (*viz.* 2 taps). This topology is passive, as it only consists of passive elements: delay lines and attenuators. The width and length of the delay lines, and attenuators are optimized to achieve a TF that is conjugately matched to the channel's TF (leakage from both the circulators). The delay spread and filter coefficients are obtained using a DE algorithm. The specific filter taps are weighted filter coefficients with values {2,2} and the delay spread is {0.042} ns at the center frequency. For optimization, we have considered several factors. A general rule for determining the population size is to multiply the number of parameters that can be optimized by 5 until the maximum number of parameters is reached (15 in this case). Smaller





TABLE 1. Performance Comparison With Current State-of-the-Art Implementations of STAR Systems

Reference	Bandwidth	Tx-Rx Isolation	Signal loss	Technology
[14]	80 MHz	50-56 dB	Low (.25 dB)	Tx and Rx loss improves at the cost of additional use of PA and hybrid couplers in RF domain.
[19]	2 GHz	45 dB	High (3 dB)	Two circulators, a balun, and a power divider are combined, but half of Tx power is lost.
[20]	300 MHz	55 dB	High (3 dB)	No circulator needed, but half of Tx power is wasted.
[21]	42 MHz	50 dB	High	19 tap filtering technique and a local oscillator were used for SIC cancellation.
[22]	107 MHz	40 dB	High (>3 dB)	An integrated six-port beamforming network (BFN) is used. More than half of the power is lost.
[23]	100 MHz	40 dB	High (>3dB)	Three Wilkinson power dividers and phase delay lines were used. A high amount of power is lost.
[24]	100 MHz	47 dB	High	Dual polarized antenna elements fed by two modified Butler matrices. Half of the power is lost.
[25]	20 MHz	35 dB	High (4.5 dB)	Three quadrature hybrids were used to create quasi-circulators.
[26]	100 MHz	65 dB	High	A directional coupler and, tuning circuits are used causing Tx power loss.
[27]	single freq.	45 dB	High	Electrical duplexer implemented with Tx insertion loss.
[29]	26 MHz	60 dB	High	Balanced feed network, but showed Tx insertion loss.
[30]	65 MHz	40 dB	High	A single circulator is used, but the implementation of the IMT at high frequencies is challenging.
[31]	10:1	39.6 dB	N/A	Photonic circulator requires perfect matching of the antenna for SIC cancellation.
This work	25 MHz	37 dB	low(1.7 dB)	Symmetrical configuration realized with two circulators and an FIR circuit causes minimal loss.

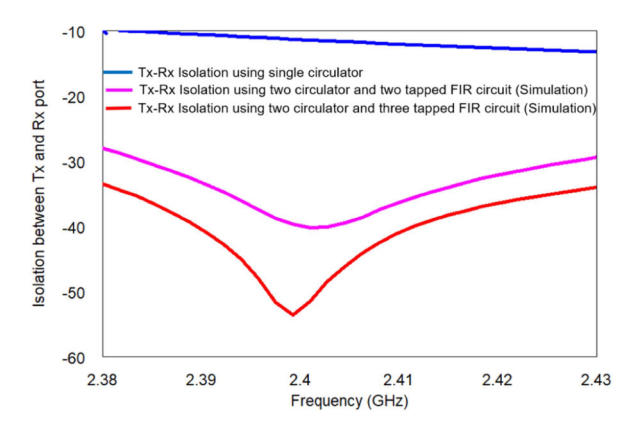


FIGURE 9. Monostatic STAR system simulation results. Clearly, our design achieves an average Tx/Rx port isolation of  $\sim$ 37 dB across a 25 MHz bandwidth (viz. 2.395-2.42 GHz).

Dual Circulators

TX pol

TX p

FIGURE 10. Fabricated prototype of the monostatic STAR system.

populations get results faster, but they are more likely to get stuck in a local optimum. No matter how many parameters there are, population sizes of more than 60 are generally unsuitable. When we tuned our circuit to imitate the coupling response, the size of our population was always less than 60.

We used the greedy technique in our SIC design since it yields results the quickest. Without a first estimate, the problem becomes more tricky. We decided to choose a larger cross-over probability as a result. The usual range of values is 0.0 to 1.0. The cross-over probability in our scenario is 0.9. We first performed circuit simulation to get the optimum weights of the circuit elements using this algorithm. The simulated performance is shown in Fig. 9. Clearly, our design achieves an average Tx/Rx port isolation of ~37 dB across a 25 MHz bandwidth (*viz.* 2.395-2.42 GHz). We also perform the simulation of our RFSIC system with three-tap FIR circuits. As can be seen, an additional 9 dB cancellation is achieved across 50 MHz. However, the three-tap FIR circuit

incorporates an additional delay line and attenuator to achieve greater cancellation.

# VI. SELF-INTERFERENCE CANCELLATION CIRCUIT FABRICATION

The monostatic SIC described in Section V was fabricated on a 0.8182 mm thick, Rogers 4003 C substrate ( $\epsilon_r = 3.38$  and  $\tan \delta = 0.0027$ ). The final prototype is shown in Fig. 10. Foremost, to evaluate the overall performance of the presented single-antenna FD system, the achieved SI cancellation was tested by measuring the amount of the Tx signal leaked to the receiver ( $S_{31}$ ). To reduce the amount of reflection, we enclosed antenna with absorbers, as depicted in Figure 11. The average measured cancellation for the system is of 36 dB across a BW of 25 MHz, which is displayed in Fig. 12. It is worth mentioning that the accuracy of the measurements is contingent on the accuracy of the attenuator values and hybrid coupler losses.

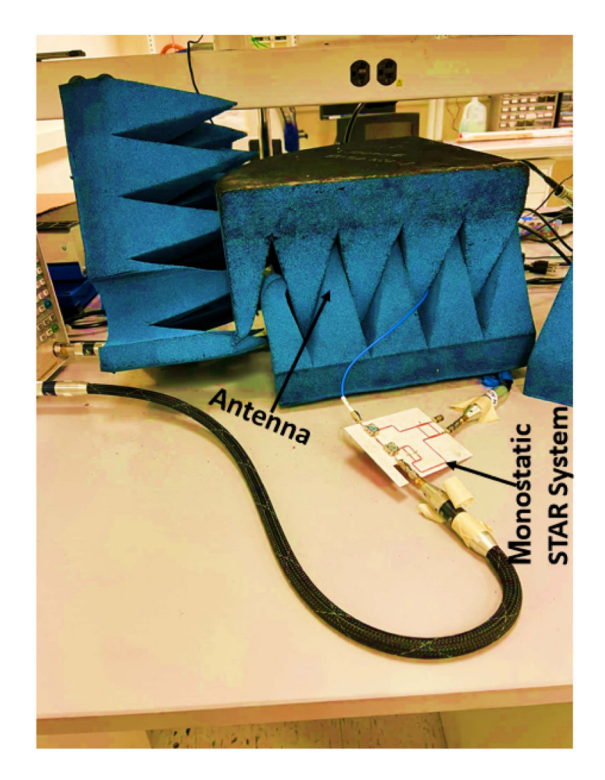


FIGURE 11. Measurement setup for testing the monostatic STAR system.

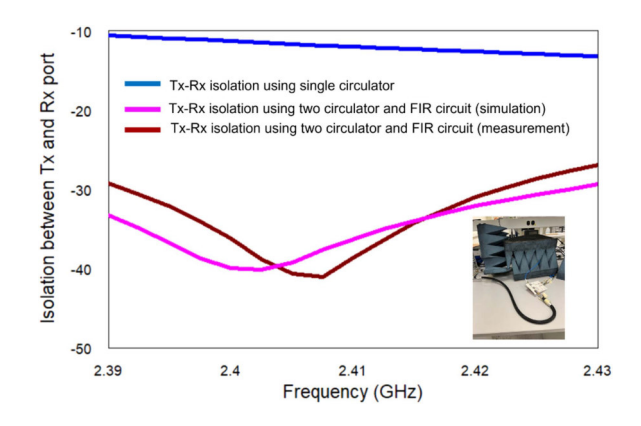


FIGURE 12. Measured vs. Simulated Tx-Rx isolation of the overall dual circulator and FIR architecture.

To evaluate our system in an active environment, we fed the Tx port with a 200 MHz modulated signal that has a power level of 0 dBm. The measurement setup is shown in Fig. 13 and its respective results in Fig. 14. These measurements indicate that an average isolation of 36 dB isolation across 25 MHz. Since our circulator operates from 2.365 to 2.435 GHz, we have designed our filter and other circuit components across these operating frequencies. We measured a maximum Tx/Rx port isolation of 42 dB and a minimum of 33 dB (on average, Tx/Rx port isolation of ~37 dB is achieved from 2.395-2.42 GHz). Therefore, our system will work with any M-ary modulation with a bandwidth up to 200 MHz.



FIGURE 13. Tx-Rx isolation testing with active measurement.

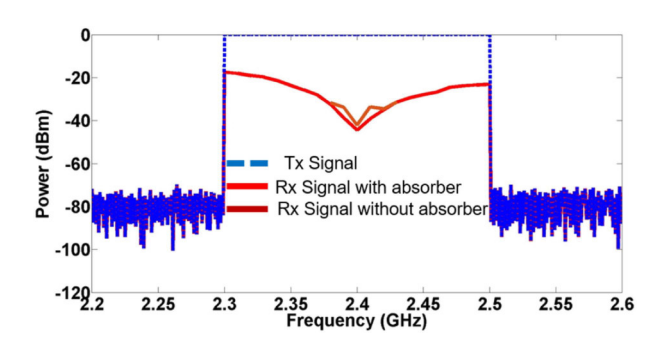


FIGURE 14. Tx-Rx signal in the monostatic STAR system showing a reduction by 36 dB across 25 MHz.

# VII. COMPARISON WITH OTHER STATE-OF-ART STAR SYSTEMS

Table 1 compares the performance of our monostatic-stage STAR implementation compares with other state-of-the-art systems presented in the literature. Initially, early monostatic STAR topologies made use of circulators in order to accomplish high isolation [19]. The most significant drawback of this approach is the loss of Tx signal caused by the component's internal leakage. When there is no circulator involved, other types of monostatic STAR implementations can achieve an isolation level of up to 55 dB [20]. For instance, by using an electrical duplex to substitute a circulator, these systems can manage to attain an isolation level of 60 dB across 26 MHz, as seen in [29]. However, a considerable amount of Tx will be lost using this approach. Another technique for monostatic systems with high isolation is beamforming. However, this beam-informing approach results in significant Tx and Rx power loss [22], [24]. Alternatively, an impedance matching terminal (IMT) circuit, like the one in [30], can be also used, and it is constructed by employing the secondary signal for the purpose of canceling the primary SI. While this work achieves 40 dB of isolation across a 65 MHz bandwidth, it must be noted that the IMT circuit requires a capacitor or an inductor, both components that are impractical for the higher





frequencies. On the other hand, we have developed and implemented a monostatic cancellation system that makes use of the symmetric coupling cancellation technique, while limiting the losses typically associated with circulator-based designs. This architecture marks the very first time that symmetry has been implemented utilizing several circuits, such as the two circulators and the FIR filter. Additionally, our FIR circuit offers low-profile characteristics as it was fabricated on a microstrip. Overall, our design can attain an average isolation of 36 dB, with a minimum of 33 dB and a maximum of 42 dB.

## **VIII. CONCLUSION**

A power-efficient, monostatic RF-SIC system based on two circulators and a filter architecture is presented. This design operates across a 25 MHz bandwidth and achieves a coupling suppression, between the transmit and receive ports, of 37 dB (with a minimum of 35 dB and a maximum of 41 dB). While the two circulators alone offered an isolation equal to 12 dB, the system's overall isolation was improved through the implementation of a symmetrical arrangement consisting of a two-tap FIR circuit and a second circulator placed in the middle. The second circulator with the filter allows for the creation of a quasi-replica of the leaked transmitted signal, that results in sufficient isolation, high power efficiency, and a minimal power loss of the Tx signal. As a result, this setup brings the overall isolation up to 41 dB, which is a significant gain. Moreover, after experimental verification, our system achieved a cancellation that was measured to be 36 dB (with a minimum of 33 dB and a maximum of 42 dB). The disparity between simulation and measurement results is mostly attributable to the fabrication tolerance, exact phase balance of the hybrid coupler, and a number of other factors. Undoubtedly, this ground-breaking monostatic STAR system is a major contender for the next generation of 5G connectivity.

## **REFERENCES**

- H. C. Papadopoulos and C.-E. Sundberg, "Reduction of mixed cochannel interference in microcellular shared time-division duplexing (STDD) systems," *IEEE Trans. Veh. Technol.*, vol. 47, no. 3, pp. 842–855, Aug. 1998.
- [2] L. Dong, "Open-loop beamforming for frequency-division duplex mobile wireless access," *IEEE Trans. Veh. Technol.*, vol. 56, no. 4, pp. 1845–1849, Jul. 2007.
- [3] S. K. Sharma, T. E. Bogale, L. B. Le, S. Chatzinotas, X. Wang, and B. Ottersten, "Dynamic spectrum sharing in 5G wireless networks with full-duplex technology: Recent advances and research challenges," *IEEE Commun. Surv. Tut.*, vol. 20, no. 1, pp. 674–707, Jan.–Mar. 2017.
- [4] M. N. Uddin and S. Choi, "Non-uniformly powered and spaced corporate feeding power divider for high-gain beam with low SLL in millimeter-wave antenna array," Sensors, vol. 17, 2020, Art. no. 4753.
- [5] Samsung Research, "6G: The next hyper-connected experience for all," Samsung, 2020.
- [6] M. N. A. Tarek, R. Hokayem, S. R. Govindarajulu, M. H. Novak, and E. A. Alwan, "A two-stage wideband RF cancellation of coupled transmit signal for bi-static simultaneous transmit and receive system," *IEEE J. Microwaves*, vol. 2, no. 3, pp. 429–441, Jul. 2022.
- [7] E. A. Etellisi, M. A. Elmansouri, and D. S. Filipovic, "Wideband monostatic simultaneous transmit and receive (STAR) antenna," *IEEE Trans. Antennas Propag.*, vol. 64, no. 1, pp. 6–15, Jan. 2016.
- [8] S. B. Venkatakrishnan, E. A. Alwan, and J. L. Volakis, "Wideband RF self-interference cancellation circuit for phased array simultaneous transmit and receive systems," *IEEE Access*, vol. 6, pp. 3425–3432, 2018.

- [9] M. N. A. Tarek, M. Novak, and E. A. Alwan, "RF coupling suppression circuit for simultaneous transmit and receive systems," in *Proc. IEEE Int. Symp. Antennas Propag. North Amer. Radio Sci. Meeting*, 2020, pp. 1833–1834, doi: 10.1109/IEEECONF35879.2020.9329641.
- [10] K. E. Kolodziej, B. T. Perry, and J. S. Herd, "In-band full-duplex technology: Techniques and systems survey," *IEEE Trans. Microw. Theory Techn.*, vol. 67, no. 7, pp. 3025–3041, Jul. 2019, doi: 10.1109/TMTT.2019.2896561.
- [11] D. Bharadia, E. McMilin, and S. Katti, "Full duplex radios," in *Proc. ACM SIGCOMM Conf. SIGCOMM*, Hong Kong, China, 2013, pp. 375–386.
- [12] I. Hwang, B. Song, C. Nguyen, and S. S. Soliman, "Digitally controlled analog wideband interference cancellation for in-device spectrum sharing and aggregation," *IEEE J. Sel. Areas Cowman*, vol. 34, no. 11, pp. 2838–2850, Nov. 2016.
- [13] D. Carsenat and C. Decroze, "UWB antennas beamforming using passive time-reversal device," *IEEE Antennas Wireless Propag. Lett.*, vol. 11, pp. 779–782, 2012.
- [14] N. Ginzberg, D. Regev, G. Tsodik, S. Shilo, D. Ezri, and E. Cohen, "A full-duplex quadrature balanced RF front end with digital pre-PA selfinterference cancellation," *IEEE Trans. Microw. Theory Techn.*, vol. 67, no. 12, pp. 5257–5267, Dec. 2019.
- [15] D. S. Filipović, M. Elmansouri, and L. Boskovic, "Full-duplex communications: Antenna story," in *Proc. 15th Int. Conf. Adv. Technol., Syst. Serv. Telecommun.*, 2021, pp. 3–6.
- [16] K. E. Kolodziej, J. G. McMichael, and B. T. Perry, "Multitap RF canceller for in-band full-duplex wireless communications," *IEEE Trans. Wireless Commun.*, vol. 15, no. 6, pp. 4321–4334, Jun. 2016.
- [17] D. Lee and B.-W. Min, "1-TX and 2-RX in-band full-duplex radio frontend with 60 dB self-interference cancellation," in *Proc. IEEE MTT-S Int. Microw. Symp.*, Phoenix, AZ, USA, 2015, pp. 1–4.
- [18] T. Dinc and H. Krishnaswamy, "A T/R antenna pair with polarization-based reconfigurable wideband self-interference cancellation for simultaneous transmit and receive," in *Proc. IEEE MTT-S Int. Microw. Symp.*, 2015, pp. 1–4.
- [19] M. Mahdi, M. Darwish, H. Tork, and A. A. Eltager, "Balun based transmitter leakage cancellation for wide-band applications," in *Proc.* 12th Int. Conf. Elect. Eng., 2020, pp. 254–257.
- [20] U. D. Silva, S. Pullipati, S. B. Venkatakrishnan, S. Bhardwaj, and A. Madanayake, "A passive STAR microwave circuit for 1-3 GHz self-interference cancellation," in *Proc. IEEE 63rd Int. Midwest Symp. Circuits Syst.*, 2020, pp. 105–108.
- [21] T. Zhang, A. Najafi, C. Su, and J. C. Rudell, "18.1 A 1.7-to-2.2 GHz full-duplex transceiver system with > 50 dB self-interference cancellation over 42 MHz bandwidth," in *Proc. IEEE Int. Solid-State Circuits Conf.*, 2017, pp. 314–315, doi: 10.1109/ISSCC.2017.7870387.
- [22] D. Wu et al., "Wideband co-polarized antenna system for in-band full-duplex applications," in *Proc. 16th Eur. Conf. Antennas Propag.*, 2022, pp. 1–4, doi: 10.1109/ISSCC.2017.7870387.
- [23] D. Wu, Y.-X. Sun, B. Wang, and R. Lian, "A compact, monostatic, cocircularly polarized simultaneous transmit and receive (STAR) antenna with high isolation," *IEEE Antennas Wireless Propag. Lett.*, vol. 19, no. 7, pp. 1127–1131, Jul. 2020, doi: 10.1109/LAWP.2020.2991182.
- [24] J. Ha, M. A. Elmansouri, P. V. Prasannakumar, and D. S. Filipovic, "Monostatic co-polarized full-duplex antenna with left- or right-hand circular polarization," *IEEE Trans. Antennas Propag.*, vol. 65, no. 10, pp. 5103–5111, Oct. 2017, doi: 10.1109/TAP.2017.2741064.
- [25] S. K. Cheung, T. P. Halloran, W. H. Weedon, and C. P. Caldwell, "MMIC-Based quadrature hybrid quasi-circulators for simultaneous transmit and receive," *IEEE Trans. Microw. Theory Techn.*,vol. 58, no. 3, pp. 489–497, Mar. 2010, doi: 10.1109/TMTT.2010.2040325.
- [26] S.-C. Jung, M.-S. Kim, and Y. Yang, "A reconfigurable carrier leak-age canceler for UHF RFID reader front-ends," *IEEE Trans. Circuits Syst. I, Reg. Papers*, vol. 58, no. 1, pp. 70–76, Jan. 2011, doi: 10.1109/TCSI.2010.2071550.
- [27] M. Mikhael, B. V. Liempd, J. Craninckx, R. Guindi, and B. Debaillie, "An in-band full-duplex transceiver prototype with an in-system automated tuning for RF self-interference cancellation," in *Proc. 1st Int. Conf. 5G Ubiquitous Connectivity*, 2014, pp. 110–115.
- [28] L. Laughlin, M. A. Beach, K. A. Morris, and J. L. Haine, "Optimum single antenna full duplex using hybrid junctions," *IEEE J. Sel. Areas Commun.*, vol. 32, no. 9, pp. 1653–1661, Sep. 2014.
- [29] M. E. Knox, "Single antenna full duplex communications using a common carrier," in *Proc. IEEE Wireless Microw. Technol. Conf.*, 2012, pp. 1–6, doi: 10.1109/WAMICON.2012.6208455.

- [30] S. Khaledian, F. Farzami, B. Smida, and D. Erricolo, "Inherent self-interference cancellation for in-band full-duplex single-antenna systems," *IEEE Trans. Microw. Theory Techn.*, vol. 66, no. 6, pp. 2842–2850, Jun. 2018, doi: 10.1109/TMTT.2018.2818124.
- [31] C. H. Cox and E. I. Ackerman, "Photonics for simultaneous transmit and receive," in *Proc. IEEE MTT-S Int. Microw. Symp.*, 2011, pp. 1–4, doi: 10.1109/MWSYM.2011.5972840.
- [32] M. N. A. Tarek, M. Roman, and E. A. Alwan, "Power efficient RF self-interference cancellation system for simultaneous transmit and receive," in *Proc. IEEE Int. Symp. Antennas Propag. USNC-URSI Radio Sci. Meeting*, 2021, pp. 113–114 doi: 10.1109/APS/URSI47566.2021.9704722.



MD NURUL ANWAR TAREK (Graduate Student Member, IEEE) received the B.E. degree in electrical and electronics engineering from the Chittagong University of Engineering and Technology, Bangladesh, in 2013, and the M.E. degree from Georgia Southern University, Statesboro, GA, USA. He is currently working toward the Ph.D. degree with Florida International University, Miami, FL, USA. He is a Research Assistant with the Smart millimeter-Wave RF Technologies Lab, Florida International University. His research in-

terests include full-duplex for 5G communication systems, millimeter wavemixers, RF front ends, and implant antennas for medicinal purposes.



MARISOL ROMAN GUERRA (Graduate Student Member, IEEE) was born in Valencia, Venezuela, in 1999. She received the B.S. degree (summa cum laude/Hons.) in electrical engineering from Florida International University, Miami, FL, USA, in 2020, where she is currently working toward the Ph.D. degree in electrical engineering. Since 2020, she has been a Graduate Research Assistant with the Smart Millimeter-Wave RF Technologies Lab with the Electrical and Computer Engineering Department, Florida International University. She is the

author of one conference paper, and a coauthor of two journals and two conference papers. Her research interests include antennas and radio frequency systems and spectrally efficient simultaneous transmit and receive communication systems. She was the recipient of the NASA Fellowship Activity since in 2020



ANTHONY NUNEZ (Graduate Student Member, IEEE) received the B.S. degree in computer engineering from Florida International University (FIU), Miami, FL, USA, in 2017, where he is currently working toward the Ph.D. degree in electrical engineering. Since 2018, he has been a Graduate Research Assistant under FIU's SmARTech Lab and Transforming Antennas Center, Miami. His research interests include physically and frequency reconfigurable filters for aerospace and commercial applications, cost saving optimizations

and rapid prototyping techniques for teaching and research, and pedagogical improvements in engineering. He is a McNair Fellow, NACME Scholar, and Braman Scholar.



MD NAZIM UDDIN (Graduate Student Member, IEEE) received the B.Sc. degree in electrical and electronic engineering from the Chittagong University of Engineering and Technology, Bangladesh, and the M.Sc. degree in electrical engineering from the University of Ulsan, Ulsan, South Korea. He is currently working toward the Ph.D. degree in electrical engineering with Florida International University, Miami, FL, USA. From 2014 to 2018, he was a R&D Engineer in a leading electronic manufacturing company in Bangladesh.

In 2021, he was an Intern with the Korea Institute of Science and Technology, Seoul, South Korea. His research interests include antenna design, mmWave antenna for 5G applications, reconfigurable beam steering using active circuits, shared aperture-aperture antenna, and tunable multiferroics small antenna.



ELIAS A. ALWAN (Member, IEEE) was born in Aitou, Lebanon, in 1984. He received the B.E. degree (summa cum laude) in computer and communication engineering from Notre Dame University—Louaize, Zouk Mosbeh, Lebanon, in 2007, the M.E. degree in electrical engineering from the American University of Beirut, Beirut, Lebanon, in 2009, and the Ph.D. degree in electrical and computer engineering from Ohio State University, Columbus, OH, USA, in 2014. He is currently an Eminent Scholar Chaired Assistant Professor with

the Electrical and Computer Engineering Department, Florida International University, Miami, FL, USA. He was a Senior Research Associate with the Electro Science Laboratory, OSU, from 2015 to 2017. His research interests include antennas and radio frequency systems with particular focus on ultrawideband (UWB) communication systems, including UWB arrays, reduced hardware and power-efficient communication back-ends, and millimeterwave technologies for 5G applications. He was the recipient of the 2020 NSF CAREER Award. He has been a Phi Kappa Phi Member since 2010.